Parametric Short-Circuit Force Analysis of Three-Phase Busbars—A Fully Automated Finite Element Approach

Dimitris G. Triantafyllidis, Petros S. Dokopoulos, *Member, IEEE*, and Dimitris P. Labridis, *Senior Member, IEEE*

***Abstract*—A three-phase busbar arrangement with straight rigid conductors carrying short-circuit currents is investigated. Calculations are made assuming steady-state ac current with a peak value equal to the peak value of the short-circuit current. The electromagnetic forces are calculated by solving the electromagnetic field diffusion equation numerically, using finite elements. The results are compared with results calculated according to the IEC Standard 865/93. A large number of arrangements have been examined, covering a wide variety of cases, as used in ac indoor installations of medium and low voltage. For this purpose, the finite element procedure has been fully automated to a degree of minimal human intervention. A let-it-grow artificial neural network (ANN) has been utilized for the automatic mesh generation. The forces calculated were in all cases in excellent agreement with the IEC Standard 865/93.**

***Index Terms*—Adaptive systems, busbars, electromagnetic forces, finite element methods, neural network applications.**

I. Introduction

SHORT-CIRCUIT currents may exert hazardous forces on busbars, especially in compact indoor installations where distances are relatively small. Therefore, a careful consideration of electromagnetic forces and their effects is needed in order to avoid excessive stresses applied on the conductors and bending moments applied on the supporting insulators. Effects of short-circuit currents are analyzed in IEC Standard 865/93 [1]. The standard is based on relations established on the well-known formula of force acting on filamentary conductors. In order to take into account the force dependency on the geometrical configuration and the profile of the conductors, an effective distance between main conductors has been introduced in [1].

A way to obtain more accurate results is to solve the electromagnetic diffusion equation, which gives the entire information for the field, current, and force distributions. Therefore, it is reasonable to compare results proposed by [1] with calculations obtained from the solution of the electromagnetic field diffusion equation using the finite element method (FEM). In [2], a short-circuit force computation based on finite elements has been presented for two busbar arrangements.

However, due to the difficulties introduced by the great number of initial finite element meshes needed to perform a full parametric analysis of such a problem, in order to compare with all the possible busbar arrangements presented in [1], an automation of the initial mesh seems very helpful. This automatically created initial mesh must be a quality mesh, in order to assure qualitative results with the minimum computational cost. In order to accomplish this, a variation [3] of a let-it-grow (LIG) artificial neural network (ANN) presented in [4] and [5] has been introduced and applied to the busbar problem. The performance of the mesh generator has been examined in terms of the short-circuit maximum force values given in [1], [2], and [6] as well as in terms of the mesh quality. The new method has also been compared with conventional FEM meshing techniques, presenting in all cases similar or better accuracy but less computational cost.

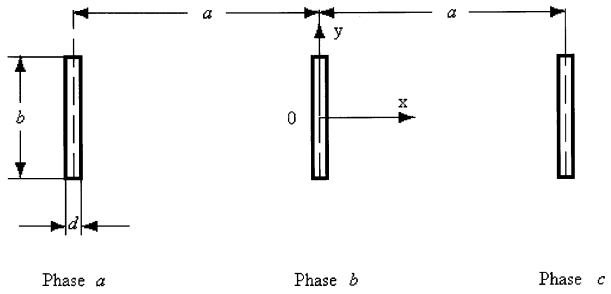

Fig. 1. Cross-section of rigid busbars.

II. Problem Description

The conventional arrangement of busbars, as shown in Fig. 1—in parallel and in a single plane—is taken as a basis for the calculations. The busbars are loaded with balanced harmonic 50-Hz currents, given in phasor notation by

$$\begin{aligned} I_a &= \sqrt{2} I_{rms} e^{j0^\circ} \\ I_b &= \sqrt{2} I_{rms} e^{-j120^\circ} \\ I_c &= \sqrt{2} I_{rms} e^{-j240^\circ}. \end{aligned} \tag{1}$$

It is assumed that

- the fault examined is a three-phase symmetrical short-circuit, because it causes the greatest dynamic stress [6];
- the center-line distance a between busbars is much smaller than the conductor length, so that the busbars can be regarded as being of infinite length, thus the problem may be considered as two dimensional;

Manuscript received June 14, 2000.

The authors are with the Power Systems Laboratory, Department of Electrical and Computer Engineering, Aristotle University of Thessaloniki, Thessaloniki, GR-54006, Greece (e-mail: dimtri@egnatia.ee.auth.gr; petros@eng.auth.gr; labridis@eng.auth.gr).

Digital Object Identifier 10.1109/TPWRD.2002.804570

0885-8977/02$17.00 © 2003 IEEE

- the magnetic permeability is constant, since copper or aluminum bars are used in installations;
- a steady state, balanced three-phase system of currents (1) is applied to the three-phase busbars, with a root-mean-square (rms) value I_{rms} obtained from the peak value of the short-circuit current i_{p3} in the case of a balanced three-phase short circuit, that is

$$I_{rms} = \frac{i_{p3}}{\sqrt{2}}. \tag{2a}$$

These assumptions have also been used in the related standard. The rms value of the current, following the last assumption, may be calculated as described in [2].

III. Mesh Generation

One of the most important steps in FEM analysis is the generation of a quality mesh, which will provide accurate and fast results for the problem in question.

One way of creating the initial mesh would be to overdiscretize the solving area, using a large number of elements. In this case though, the computing resources are not exploited properly, since large amounts of memory and computation time are required. Also, error buildup, due to the unnecessary large number of elements, may lead to inaccurate results.

Another approach is to start the solving process by using an initial coarse mesh and to refine it afterwards by means of an adaptive meshing procedure [7], [8]. During this procedure, the solution error is estimated for each element and the elements with error exceeding a given threshold are split into smaller ones. This way, the initial mesh is refined and the procedure is repeated, until the needed accuracy is met. This technique will provide very accurate results, but is quite time and memory consuming. Also, it does not take into account the experience that may have already been obtained by solving similar problems. In many cases, an experienced user may be able to foresee the density that the final mesh should have.

In the present paper, a variation of an LIG ANN-[9] based mesh generator has been utilized [3]–[5] in order to ensure qualitative results with less computational cost. An initial mesh of 1500 nodes is provided by the LIG ANN as a starting point for the adaptive meshing procedure, which will refine the original mesh. In this technique, the number of nodes (neurons) of the LIG ANN grows with time, while trying to adapt itself to a given mesh density function.

The first step in the mesh generation procedure is to create an initial mesh that will be used as a starting point for the LIG-based mesh generator and as a sample point grid for the mesh density prediction. This initial mesh has been devised as follows: starting from a constrained delaunay triangulation (CDT) [10] of the solving area (Figs. 2 and 3), the triangles are subdivided into smaller triangles until a geometric constrain is met, which in this case was that no neighboring triangles may differ in an area more than a factor of 4.5. Thus, a graded mesh is provided, shown in Figs. 5 and 6.

The second step is to estimate the mesh density for the problem to be solved. This can be done by training an ANN

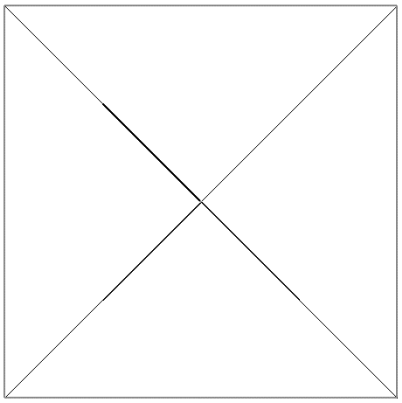

Fig. 2. CDT of the solving region ($b/d = 3$, $a/d = 3$).

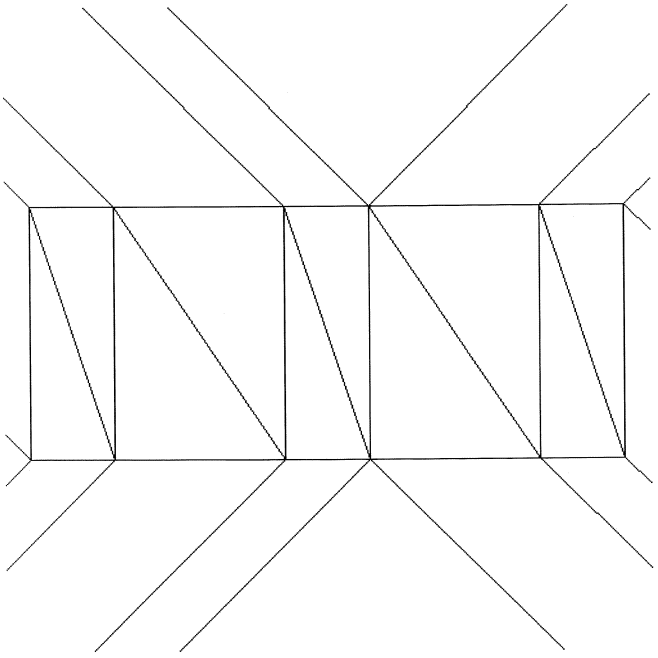

Fig. 3. CDT of Fig. 2 in the conductor's neighborhood.

to be able to reproduce the mesh density vector of a family of problems [11]–[13] or the mesh density vector may be provided by the user in some cases. In the present work, another approach has been selected for its simplicity, efficient accuracy, and speed. The mesh density inside each triangle of the graded mesh has been estimated by calculating the intensity of the magnetic field $H(r, t)$ at the barycentres of the respective triangles, using Ampere's law, where r is the distance between the busbar center and the respective barycentre. For the magnetic field inside the busbars, circular conductors with the same cross-section as the rectangular busbars have been assumed. Also, the current $i(t)$ has been considered to have a uniform distribution over the conductor's area resulting in (2b)

$$H(r, t) = \begin{cases} \dfrac{i(t)}{2bd} \cdot r & \text{for triangles inside the busbars} \\ \dfrac{i(t)}{2\pi r} & \text{for triangles outside the busbars.} \end{cases} \tag{2b}$$

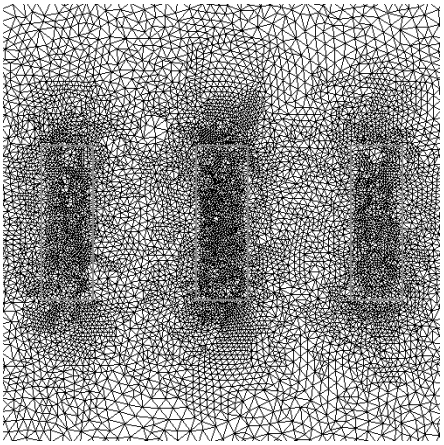

Fig. 4. Starting from the CDT of Fig. 2, this mesh was produced after 19 adaptive refinements.

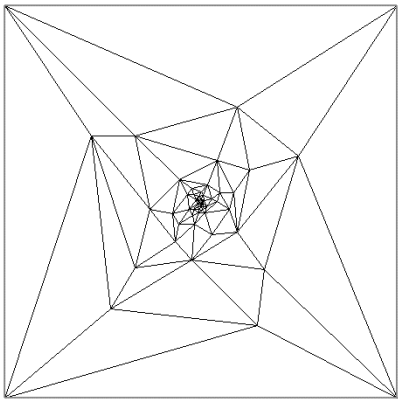

Fig. 5. Graded mesh of the solving region ($b/d = 3$, $a/d = 3$).

Although this introduces an error, especially in cases where b/d is far from unity, it is acceptable for two reasons: a) the calculation of the magnetic field in this step is only a rough estimate in order to predict the mesh density; and b) the initial mesh is used only as a starting point in an adaptive mesh refinement process, which will improve the initial mesh further. The magnetic field at a given point has been calculated as the superposition of the magnetic field due to the three-phase currents (1) flowing in the three busbars. Since the magnetic field H is time-dependent, in order to achieve a proper mesh density prediction, the values of $i(t)$ for three different time moments, corresponding to an angle difference of 120°, have been averaged.

The next step in the mesh generation process, once the mesh density has been estimated, is to produce a mesh that is denser at the required regions by means of the LIG-based mesh generator (Figs. 8 and 9). At last, a Delaunay triangulation takes place. In order to improve mesh quality even further, the nodes of the triangles are moved toward the centroid of the polygon, formed by their respective neighboring nodes [8]. The produced mesh is then refined with the adaptive procedure of [14], using as local error estimator the discontinuity of the instantaneous tangential components of the magnetic field (Fig. 10).

For reasons of comparison, two conventional meshing procedures have also been applied for the solution of the same busbar problem. In the first case, an initial CDT of the solving region has been refined using the same adaptive meshing procedure of [14]. In the second case, the graded mesh shown in Figs. 5 and 6, used as a starting point in the first step of the LIG mesh generation procedure, has also been refined [14]. Figs. 4 and 7 present the corresponding final meshes.

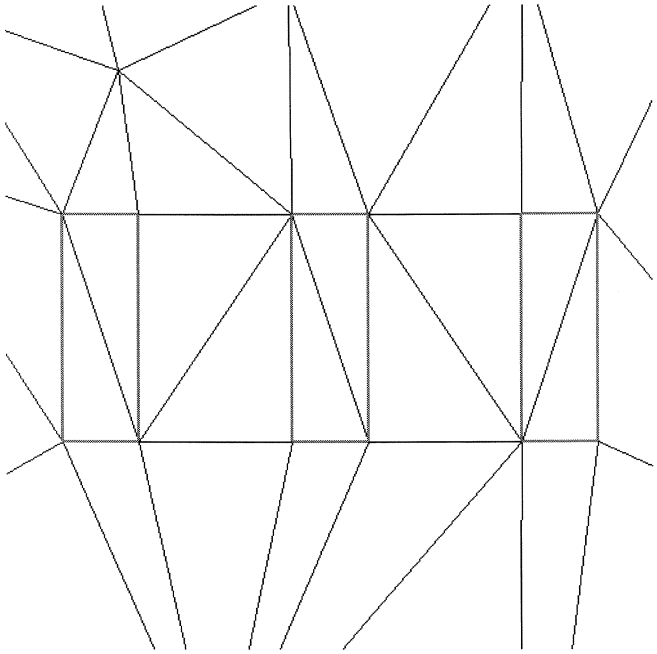

Fig. 6. Graded mesh of Fig. 5 in the conductors' neighborhood.

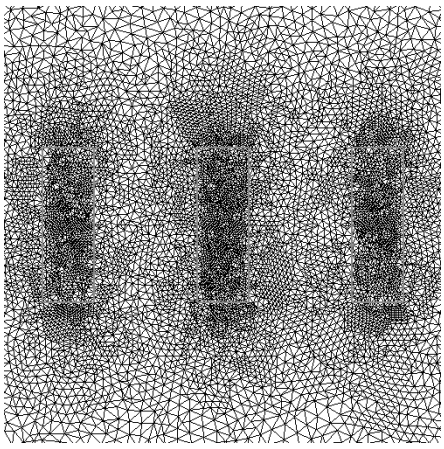

Fig. 7. Starting from the graded mesh of Fig. 5, this mesh was produced after seven adaptive refinements.

IV. Computation of Short-Circuit Forces

A. Calculations According to IEC Standard 865/93

The forces acting on the busbars of Fig. 1 carrying short-circuit currents depend on the geometrical configuration and the profile of the busbars. For this reason, an effective distance a_m is introduced in [1] and the maximum force per unit length F_{mb}, acting on the central conductor (phase b) of Fig. 1 is given by

$$F_{mb} = \frac{\mu_0}{2\pi a_m} \frac{\sqrt{3}}{2} i_{p3}^2. \tag{3a}$$

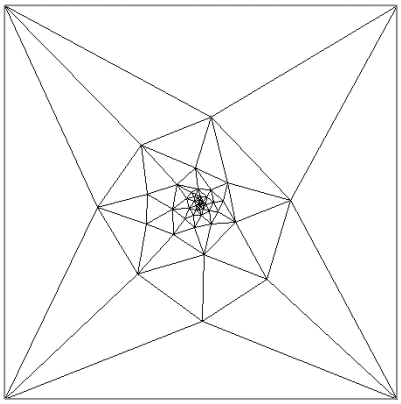

Fig. 8. Mesh produced by the LIG mesh generator ($b/d = 3$, $a/d = 3$).

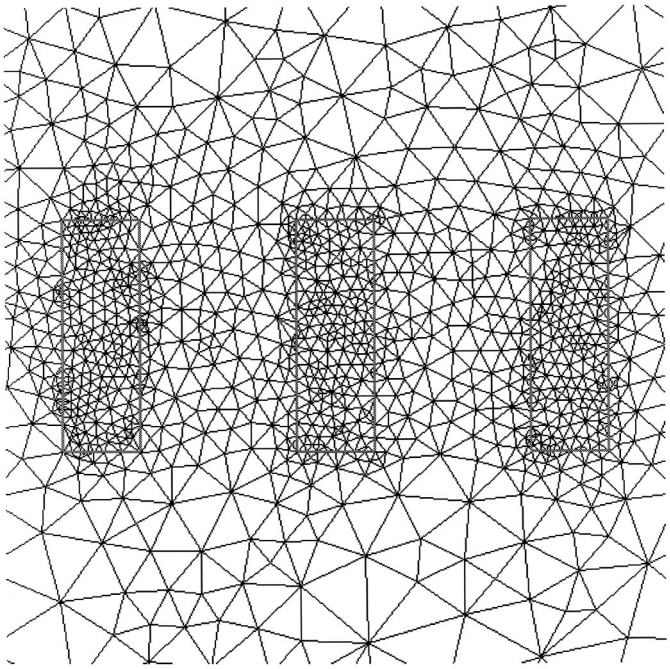

Fig. 9. Mesh produced by the LIG mesh-generator (Fig. 8) in the conductor's neighborhood.

The effective distance a_m is defined by

$$a_m = \frac{a}{k_{1s}} \tag{3b}$$

in which the factor k_{1s} may be computed from [1, Fig. 1] or alternatively from an equation given in [1, Annex A]. This factor is computed in [1] for a wide range of the geometrical parameters a, b, and d of Fig. 1, as shown in Fig. 11. It must be noted that the maximum force per unit length F_{mb} acting on the central conductor of Fig. 1 only is reported in [1], since minor forces act on the outer two main conductors. However, the maximum forces F_{ma} and F_{mc} acting on the two outer conductors may be calculated from the corresponding relations given in [2] and [6], making use of the same effective distance a_m

$$F_{ma} = F_{mc} = \frac{\mu_0}{2\pi a_m} \frac{3+2\sqrt{3}}{8} i_{p3}^2. \tag{4}$$

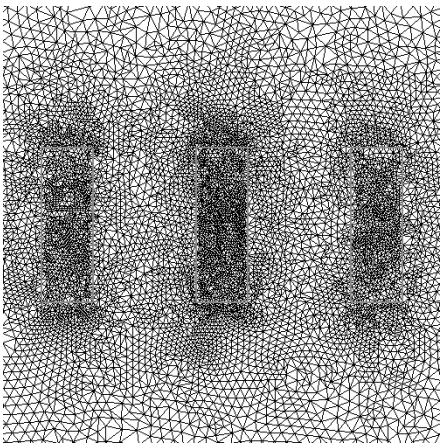

Fig. 10. Starting from the LIG mesh of Fig. 8, this mesh was produced after four adaptive refinements.

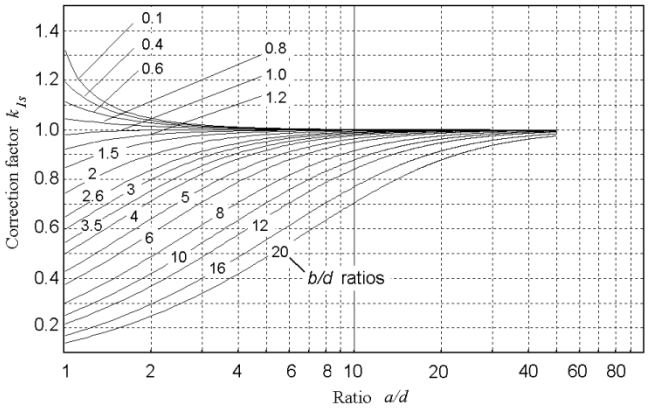

Fig. 11. Correction factor k_{1s} according to [1].

B. FEM Calculations

The maximum forces per unit length calculated by FEM follow the approach presented in [2]. The corresponding maximum force per unit length $F_{mb\,FEM}$ acting on the central conductor is associated to a correction factor k_{FEM}, using a relation similar to (3a)

$$F_{mb\,FEM} = \frac{\mu_0}{2\pi a} k_{FEM} \frac{\sqrt{3}}{2} i_{p3}^2. \tag{5}$$

The factor k_{FEM} is calculated in this paper from (5) using the FEM force results $F_{mb\,FEM}$, for the same range of the geometrical parameters a, b, and d as in [1]. This factor is accordingly compared to the corresponding factor k_{1s} shown in Fig. 11.

V. Parametrical Analysis of Forces

For the range of rigid busbar arrangements presented in [1], a parametrical analysis took place in order to produce a sufficient number of calculation points, for which the correction factor k_{FEM} was calculated. The height over width ratio b/d varied over the following values: 0.1, 0.4, 0.6, 0.8, 1.0, 1.2, 1.5, 2.0, 2.6, 3.0, 3.5, 4.0, 5.0, 6.0, 8.0, 10.0, 12.0, 16.0 and 20.0. For each of these b/d ratios, 16 a/d ratios have been chosen and the

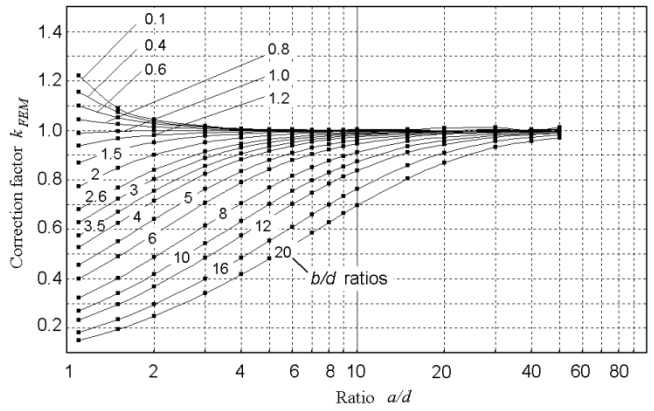

Fig. 12. Correction factor k_{FEM}, as a result of FEM analysis.

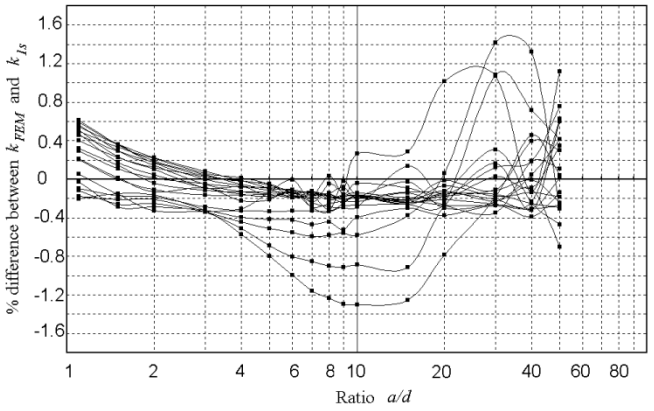

Fig. 13. Percentage difference between k_{FEM} and k_{1s} for the corresponding sample points of Fig. 12.

corresponding maximum forces were calculated by FEM solution, leading to a total of 304 calculation points. The resultant correction factor k_{FEM} is depicted in Fig. 12.

In Fig. 13, the corresponding percentage difference (7) between the two correction factors k_{FEM} and $k_{1s}$is presented

$$\%\, difference = \frac{k_{FEM} - k_{1s}}{k_{1s}} \cdot 100. \tag{7}$$

As can be seen, the differences between the results obtained by the FEM and the IEC standard are minimal. In the majority of cases, the difference is constrained within a small zone of $\pm 1\%$, while the maximum difference that occurs is less than 1.5%.

Tables I–III present data on the convergence of the FEM for all three meshing techniques described for a test case with $b/d = 3$ and $a/d = 3$. The presented mesh quality concerns the whole mesh and has been calculated by averaging [8] the mesh quality q_i of all the triangles in the mesh [15]

$$q_i = \frac{8(s - l_1)(s - l_2)(s - l_3)}{l_1\, l_2\, l_3} \tag{8}$$

where l_1, l_2, and l_3 are the lengths of the three sides of triangle i and $2s$ is its perimeter.

Table IV shows another test case ($b/d = 1$ and $a/d = 7$). In this case, the LIG mesh produces symmetrical results, concerning the calculated maximum forces acting on the left and right busbars, while the graded mesh appears to produce less symmetrical results with a larger number of nodes and more CPU time.

TABLE I
CONVERGENCE OF THE LIG PRODUCED MESH ($b/d = 3$, $a/d = 3$)

Iteration	CPU time [sec]	Nodes	Mesh quality	$F_{ma\ FEM}$ [N/m]	$F_{mb\ FEM}$ [N/m]	$F_{mc\ FEM}$ [N/m]
Initial mesh generation	37					
1	41	1500	0.894	18.78933	20.07681	18.52834
2	44	2464	0.873	19.20573	20.36448	19.06490
3	73	4797	0.869	19.33907	20.46090	19.22537
4	214	10290	0.869	19.39928	20.49821	19.29553
Total time:	**409**					

TABLE II
CONVERGENCE OF THE INITIALLY GRADED MESH ($b/d = 3$, $a/d = 3$)

Iteration	CPU time [sec]	Nodes	Mesh quality	$F_{ma\ FEM}$ [N/m]	$F_{mb\ FEM}$ [N/m]	$F_{mc\ FEM}$ [N/m]
Initial mesh generation	5					
1	23	172	0.576	12.99382	16.88919	14.07028
2	23	230	0.543	15.13697	18.00816	14.54716
3	23	340	0.665	17.97006	19.96983	17.42514
4	26	606	0.801	18.88265	20.22179	18.50463
5	30	1197	0.827	19.21018	20.33703	19.07069
6	41	2483	0.848	19.30252	20.42241	19.18526
7	80	5352	0.858	19.35454	20.48025	19.26897
8	270	11873	0.866	19.40670	20.50437	19.31088
Total time:	**521**					

TABLE III
CONVERGENCE OF THE CDT MESH ($b/d = 3$, $a/d = 3$)

Iteration	CPU time [sec]	Nodes	Mesh quality	$F_{ma\ FEM}$ [N/m]	$F_{mb\ FEM}$ [N/m]	$F_{mc\ FEM}$ [N/m]
Initial mesh generation	0.2					
1	27	16	0.477	1.26E-04	1.09E-04	1.26E-04
2	23	26	0.463	3.77E-04	3.26E-04	3.77E-04
3	23	36	0.458	1.13E-03	9.79E-04	1.13E-03
4	22	48	0.453	3.39E-03	2.94E-03	3.39E-03
5	23	60	0.450	1.02E-02	8.81E-03	1.02E-02
6	23	72	0.448	3.05E-02	2.64E-02	3.05E-02
7	23	84	0.447	9.15E-02	7.91E-02	9.14E-02
8	23	96	0.446	0.273311	0.235989	0.272643
9	23	109	0.447	0.812858	0.696103	0.805103
10	23	132	0.457	2.375314	1.999131	2.327407
11	23	159	0.470	6.640077	5.313483	6.222617
12	23	190	0.541	14.02218	11.58954	13.85215
13	25	251	0.665	14.04145	17.91932	15.41629
14	25	363	0.705	17.70305	19.38733	16.88008
15	27	618	0.739	18.75532	20.17455	18.49020
16	31	1198	0.809	19.12150	20.30374	19.04932
17	43	2469	0.833	19.29543	20.42462	19.18161
18	79	5339	0.850	19.37677	20.48431	19.25739
19	287	11655	0.868	19.40896	20.50352	19.30123
Total time:	**796.2**					

TABLE IV
SYMMETRICAL RESULTS OBTAINED BY FEM USING THE LIG PRODUCED MESH ($b/d = 1$, $a/d = 7$)

Initial mesh type	Iterations	Total CPU time [sec]	Nodes	$F_{ma\ FEM}$ [N/m]	$F_{mb\ FEM}$ [N/m]	$F_{mc\ FEM}$ [N/m]
LIG	4	289	7037	9.201887	9.868924	9.176751
Graded	7	329	7493	9.091479	9.886826	9.258652
CDT	8	638	8595	9.195296	9.890190	9.213570

TABLE V
REFERENCE VALUES FOR MAXIMUM FORCES ACCORDING TO (3a), (3b), AND (4), FOR THE TWO TEST CASES PRESENTED IN TABLES I–IV

	F_{ma} [N/m]	F_{mb} [N/m]	F_{mc} [N/m]
b/d=3, a/d=3	19.11392	20.48624	19.11392
b/d=1, a/d=7	9.23430	9.89730	9.23430

TABLE VI
PERCENTAGE DIFFERENCE BETWEEN MAXIMUM REFERENCE FORCES OF TABLE V AND THOSE OBTAINED BY FEM USING THE THREE MESHING TECHNIQUES, FOR THE TWO TEST CASES PRESENTED IN TABLES I–IV

Initial mesh type	Test case b/d=3, a/d=3			Test case b/d=1, a/d=7		
	Phase			Phase		
	a	b	c	a	b	c
LIG	1.49	0.06	0.95	-0.35	-0.28	-0.62
Graded	1.53	0.09	1.03	-1.54	-0.10	0.26
CDT	1.54	0.08	0.98	-0.42	-0.07	-0.22

For reasons of comparison, the corresponding maximum force per unit length F_{mb} acting on the middle busbar has been calculated using (3a) and (3b), while $F_{ma} = F_{mc}$ have been calculated from (4). These values, shown in Table V, are taken as a reference. The respective percentage differences between these reference values and the maximum force values obtained by FEM with the three meshing techniques are presented in Table VI, for both test cases.

As can be seen, the LIG-based meshes produce qualitative results, equivalent to or better than those obtained by using more conventionally produced meshes, like a graded or a CDT mesh. Compared to the CDT mesh, the LIG mesh introduces a significant reduction in calculation time in the order of 50%, while compared to the graded mesh, the reduction in solving time is in the range of 20%. In similar parametric calculations, where a large number of cases are being examined as part of a parametrical analysis, this reduction in solving time may be of significant interest, which justifies the amount of effort put in the development of the proposed method.

In all mentioned cases, the applied current I_{rms}, defined in (2a), had a value of 1000 A. The computations have been made using a Pentium computer at 200 MHz having 80 MB of memory, running a Linux operating system. The presented LIG mesh generator has been easily incorporated in the FEM package [14] developed at the Power Systems Laboratory of the Aristotle University of Thessaloniki, during the last 15 years.

VI. CONCLUSIONS

The FEM has been used in a parametrical analysis of rigid-busbar short-circuit force calculation. For this purpose, an automatic mesh generator was implemented, based on a let-it-grow ANN. A large variety of busbar arrangements has automatically been solved using FEM with the proposed meshing technique. Forces calculated have been compared to those obtained from the corresponding IEC 865/1993 standard, resulting in minimal differences between the two methods. In order to highlight the benefit of the proposed mesh generator, two other conventional meshing procedures have also been used with FEM. The quality meshes produced by the proposed mesh generator made the convergence of the method faster and, in some cases, led to more accurate results than the meshes produced by the conventional meshing procedures.

REFERENCES

[1] IEC-Publ. 865/1993, "Short-circuit currents—Calculation of effects. Part 1: Definitions and calculation methods," Bureau Central de la CEI, Geneve/Suisse.
[2] D. P. Labridis and P. S. Dokopoulos, "Electromagnetic forces in three-phase rigid busbars with rectangular cross-sections," *IEEE Trans. Power Delivery*, vol. 11, pp. 793–800, Apr. 1996.
[3] D. G. Triantafyllidis and D. P. Labridis, "A finite element mesh generator based on growing neural networks," *IEEE Trans. Neural Networks*, vol. 13, pp. 1482–1496, Nov. 2002.
[4] S. Alfonzetti, S. Cavalieri, S. Coco, and M. Malgeri, "Automatic mesh generation by the Let-It-Grow Neural Network," *IEEE Trans. Magn.*, vol. 32, pp. 1349–1352, May 1996.
[5] S. Alfonzetti, "A finite element mesh generator based on an adaptive neural network," *IEEE Trans. Magn.*, vol. 34, pp. 3363–3366, Sept. 1998.
[6] G. Hosemann and D. Tsanakas, "Dynamic short-circuit stress of busbar structures with stiff conductors. Parametric studies and conclusions for simplified calculation methods," *Electra*, no. 68, pp. 37–64, 1980.
[7] Z. J. Cendes and D. N. Shenton, "Adaptive mesh refinement in the finite element computation of magnetic fields," *IEEE Trans. Magn.*, vol. 21, pp. 1811–1816, Sept. 1985.
[8] N. Golias and T. Tsiboukis, "Adaptive refinement in 2-D finite element applications," *Int. J. Numer. Mod., Electr. Dev. Fields*, vol. 4, pp. 81–95, 1991.
[9] B. Fritzke, "Wachsende Zellstrukturen - ein selbstorganizierendes neuronales Netzwerkmodell," Ph.D. dissertation, Univ. Erlangen-Nürnberg, 1992.
[10] J. R. Shewchuk, "Triangle: Engineering a 2D quality mesh generator and delaunay triangulator," in *First Workshop on Applied Computational Geometry*. Philadelphia, PA: Association for Computing Machinery, 1996, pp. 124–133.
[11] D. N. Dyck and D. A. Lowther, "Determining an approximate finite element mesh density using neural network techniques," *IEEE Trans. Magn.*, vol. 28, pp. 1767–1770, Mar. 1992.
[12] R. Chedid and N. Najjar, "Automatic finite-element mesh generation using artificial neural networks—Part I: Prediction of mesh density," *IEEE Trans. Magn.*, vol. 32, pp. 5173–5178, Sept. 1996.
[13] D. G. Triantafyllidis and D. P. Labridis, "An automatic mesh generator for handling small features in open boundary power transmission line problems using artificial neural networks," *Communications in Numerical Methods in Engineering*, vol. 16, pp. 177–190, 2000.
[14] D. P. Labridis, "Comparative presentation of criteria used for adaptive finite element mesh generation in multiconductor eddy current problems," *IEEE Trans. Magn.*, vol. 36, pp. 267–280, Jan. 2000.
[15] D. A. Lindholm, "Automatic triangular mesh generation on surfaces of polyhedra," *IEEE Trans. Magn.*, vol. MAG-19, pp. 2539–2542, Nov. 1983.

Dimitris G. Triantafyllidis was born in Stuttgart, Germany, on September 25, 1972. He received the Dipl. Eng. degree from the Department of Electrical and Computer Engineering at the Aristotle University of Thessaloniki, Greece, in 1996. He is currently pursuing the Ph.D. degree at the Aristotle University of Thessaloniki. His research interests include finite elements and power systems engineering.

Mr. Triantafyllidis is a member of the Society of Professional Engineers of Greece.

Petros S. Dokopoulos (M'77) was born in Athens, Greece, on September 16, 1939. He received the Dipl. Eng. degree from the Technical University of Athens in 1962 and the Ph.D. degree from the University of Brunswick, Germany, in 1967.

Currently, he is Full Professor at the Department of Electrical Engineering at the Aristotle University of Thessaloniki, Greece, where he has been since 1978. From 1962 to 1967, he was with the Laboratory for High Voltage and Transmission at the University of Brunswick, Germany, and from 1967 to 1974, he was with the Nuclear Research Center, Julich, Germany. He was also with the Joint European Torus from 1974 to 1978. He was a Consultant with Brown Boveri and Cie, Mannheim, Germany; Siemens, Erlagen, Germany;, Public Power Corporation, Greece; and National Telecommunication Organization and construction companies in Greece. His research interests are dielectrics, power switches, power generation (conventional and fusion), transmission, distribution, and control in power systems. Dr. Dokopoulos has been published many times and holds seven patents on these subjects.

Dimitris P. Labridis (S'88–M'90–SM'00) was born in Thessaloniki, Greece, on July 26, 1958. He received the Dipl.-Eng. and Ph.D. degrees from the Department of Electrical Engineering at the Aristotle University of Thessaloniki, Greece, in 1981 and 1989, respectively.

Currently, he is an Assistant Professor in the Department of Electrical Engineering at the Aristotle University of Thessaloniki, Greece. From 1982 to 1993, he was a Research Assistant and Lecturer with the Department of Electrical Engineering at the Aristotle University of Thessaloniki. His research interests include power system analysis with special emphasis on the simulation of transmission and distribution systems, electromagnetic and thermal field analysis, numerical methods in engineering, and artificial intelligence applications in power systems.